# Hydrogen-limited growth of hyperthermophilic methanogens at deep-sea hydrothermal vents

Helene C. Ver Eecke[a], David A. Butterfield[b], Julie A. Huber[c], Marvin D. Lilley[d], Eric J. Olson[d], Kevin K. Roe[b], Leigh J. Evans[e], Alexandr Y. Merkel[f], Holly V. Cantin[c], and James F. Holden[a,1]

[a]Department of Microbiology, University of Massachusetts, Amherst, MA 01003; [b]Joint Institute for the Study of the Atmosphere and Ocean and [d]School of Oceanography, University of Washington, Seattle, WA 98195; [c]Josephine Bay Paul Center, Marine Biological Laboratory, Woods Hole, MA 02543; [e]Cooperative Institute for Marine Resources Studies, Oregon State University, Newport, OR 97365; and [f]Winogradsky Institute of Microbiology, Russian Academy of Sciences, Moscow 117312, Russia

Edited by David M. Karl, University of Hawaii, Honolulu, HI, and approved June 29, 2012 (received for review April 21, 2012)

**Microbial productivity at hydrothermal vents is among the highest found anywhere in the deep ocean, but constraints on microbial growth and metabolism at vents are lacking. We used a combination of cultivation, molecular, and geochemical tools to verify pure culture $H_2$ threshold measurements for hyperthermophilic methanogenesis in low-temperature hydrothermal fluids from Axial Volcano and Endeavour Segment in the northeastern Pacific Ocean. Two *Methanocaldococcus* strains from Axial and *Methanocaldococcus jannaschii* showed similar Monod growth kinetics when grown in a bioreactor at varying $H_2$ concentrations. Their $H_2$ half-saturation value was 66 μM, and growth ceased below 17–23 μM $H_2$, 10-fold lower than previously predicted. By comparison, measured $H_2$ and $CH_4$ concentrations in fluids suggest that there was generally sufficient $H_2$ for *Methanocaldococcus* growth at Axial but not at Endeavour. Fluids from one vent at Axial (Marker 113) had anomalously high $CH_4$ concentrations and contained various thermal classes of methanogens based on cultivation and *mcrA*/*mrtA* analyses. At Endeavour, methanogens were largely undetectable in fluid samples based on cultivation and molecular screens, although abundances of hyperthermophilic heterotrophs were relatively high. Where present, *Methanocaldococcus* genes were the predominant *mcrA*/*mrtA* sequences recovered and comprised ∼0.2–6% of the total archaeal community. Field and coculture data suggest that $H_2$ limitation may be partly ameliorated by $H_2$ syntrophy with hyperthermophilic heterotrophs. These data support our estimated $H_2$ threshold for hyperthermophilic methanogenesis at vents and highlight the need for coupled laboratory and field measurements to constrain microbial distribution and biogeochemical impacts in the deep sea.**

It is estimated that perhaps a third [56–90 petagrams (Pg)] of the Earth's total bacterial and archaeal carbon (106–333 Pg) exists within marine subsurface sediments (1–3). These global estimates do not include microbial carbon in igneous ocean crust, wherein an additional 200 Pg of carbon has been proposed to exist primarily within its porous extrusive layer (layer 2A), where hydrothermal fluids circulate through basalt as old as 65 Ma (4). Therefore, microbes in marine sediments and ocean crust have the potential to have a significant impact on biogeochemical fluxes and carbon cycles in the deep ocean. Methanogenesis and sulfate reduction are often the predominant anaerobic microbial processes in many deep subsurface marine sediments, especially near continental margins (5, 6), and methanogens and sulfate reducers are also frequently found in deep subsurface terrestrial basalts (7–9). However, models of the rates and constraints of various aerobic and anaerobic biogeochemical processes in deep subsurface environments, especially within hard rock, are nascent because of these environments being difficult to access. This has generated interest in quantitatively modeling habitability and biogeochemical processes within the deep subsurface using bioenergetic predictions of microbial metabolism, based on the supply of geochemical energy and the metabolic energy demand of the organisms (10–13).

Deep-sea hydrothermal vents are among the most productive regions within igneous ocean crust and provide a starting point for modeling subseafloor microbial processes associated with hydrothermal circulation in basalt. Thermophilic and hyperthermophilic methanogens belonging to the order Methanococcales are commonly found autotrophs in vent environments (14–21). These organisms anaerobically convert $H_2$ and $CO_2$ into biomass, $CH_4$ and $H_2O$. Limited data suggest that the abundances of methanogens and the extent of methanogenic fluid chemistry alteration are elevated in ultramafic vent sites, where serpentinization leads to high $H_2$ concentrations (16, 19–21), and at volcanic eruption sites, where posteruption $H_2$ is also more abundant (14, 22–25). In contrast, methanogen abundances and fluid alterations are often low to undetectable in other midocean ridge and volcanic arc hydrothermal systems, where $H_2$ concentrations are also relatively low (20, 26–29). This pattern of $H_2$-limited methanogenesis generally fits those predicted in bioenergetic models (11, 13), but the temperature-dependent maintenance energy data used for these models lack data for methanogenesis and all other anaerobic metabolisms above 65 °C (30). Without empirically determined growth kinetic constraints, $H_2$ availability cannot be shown definitively to be a key factor driving methanogen abundance and distribution at thermophilic growth temperatures in vent systems.

The purposes of this study were to define the Monod growth kinetics on $H_2$ and minimum $H_2$ concentrations required for the growth of *Methanocaldococcus jannaschii* and two *Methanocaldococcus* species isolated from deep-sea hydrothermal vents at Axial Volcano, strains JH146 and JH123. Sequencing and quantitative PCR (qPCR) analysis were used to determine the diversity and abundance of methanogen-specific methyl coenzyme M reductase (*mcrA*) genes in low-temperature vent fluids from Axial Volcano and nearby Endeavour Segment. The abundances of thermophilic and hyperthermophilic methanogens and hyperthermophilic heterotrophs were determined using culture-dependent techniques from the same fluids. Finally, these data were correlated with fluid geochemistry from the two sites, as well as with methanogen abundance and geochemical data from vent sites worldwide, to link our predictions of high-temperature methanogenesis with in situ measurements.

Author contributions: H.C.V., D.A.B., J.A.H., and J.F.H. designed research; H.C.V., D.A.B., J.A.H., E.J.O., K.K.R., L.J.E., A.Y.M., H.V.C., and J.F.H. performed research; H.C.V., D.A.B., J.A.H., M.D.L., and J.F.H. analyzed data; and H.C.V., D.A.B., J.A.H., and J.F.H. wrote the paper.

The authors declare no conflict of interest.

This article is a PNAS Direct Submission.

Freely available online through the PNAS open access option.

Data deposition: The sequences reported in this paper have been deposited in the GenBank database (accession nos. HQ635140–HQ635763).

[1]To whom correspondence should be addressed. E-mail: jholden@microbio.umass.edu.

This article contains supporting information online at www.pnas.org/lookup/suppl/doi:10.1073/pnas.1206632109/-/DCSupplemental.

## Results and Discussion

**Growth Kinetics and $H_2$ Limitation of *Methanocaldococcus* spp.** Three hyperthermophilic *Methanocaldococcus* species were grown in a gas flow-controlled bioreactor at either 82 °C or 70 °C to determine the effect of $H_2$ concentration on growth. Two of the organisms (JH146 and JH123) had been purified from low-temperature hydrothermal fluids collected at Axial Volcano in 2008. The third organism was the commercially available *M. jannaschii* DSM 2661 strain. All three organisms had longer doubling times and lower maximum cell concentrations with decreasing $H_2$ concentrations (Fig. 1 and Fig. S1). The minimum $H_2$ concentration for the growth of *M. jannaschii* was between 17 μM and 23 μM (Fig. 1*A*), whereas the minimum concentration for strains JH146 (Fig. 1*B*) and JH123 (Fig. S1) was between 10 μM and 17 μM. Statistically, there was no difference in the $H_2$-dependent Monod growth kinetic parameters, namely, the growth rate half-saturation constant ($K_s$) and maximum growth rate ($\mu_{max}$), for the three organisms (Fig. 1*C*). The $K_s$ for the pooled data for all three strains was 66 μM. The effect of hydrostatic pressure on our minimum $H_2$ and $K_s$ estimates was not tested. Pressure has a very minor effect on values of standard molal Gibbs energy ($\Delta G_r^\circ$) for reactions occurring in the aqueous phase (11, 31). Growth rates and hydrogenase activities of *M. jannaschii* increased modestly with pressure (32–34). However, it is not known whether pressure significantly affects the organism's affinity for aqueous $H_2$, and this is area for future research.

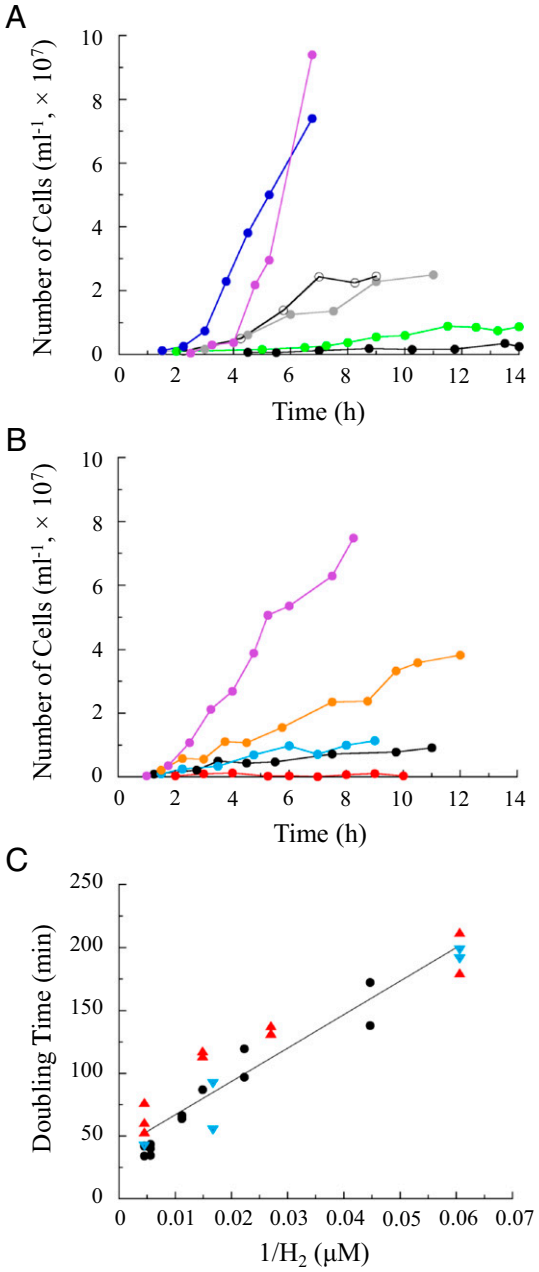


**Fig. 1.** Growth of *M. jannaschii* (*A*) and *Methanocaldococcus* strain JH146 (*B*) at 82 °C on $H_2$ concentrations of 10 μM (solid red circle), 16.5 μM (solid black circle), 22.5 μM (solid green circle), 37 μM (solid turquoise circle), 45 μM (solid gray circle), 67 μM (solid orange circle), 90 μM (open black circle), 180 μM (solid blue circle), and 225 μM (solid purple circle). (C) Monod growth kinetic plot for *M. jannaschii* (solid black circle) and strain JH146 (solid red triangle) at 82 °C and strain JH123 (solid turquoise triangle) at 70 °C.

In comparison, the $H_2$ $K_s$ values for the mesophilic methanogens *Methanospirillum hungatei* and *Methanobacterium bryantii*, each grown at 37 °C, were 6.6 μM and 18 μM, respectively (35, 36), and the minimum $H_2$ threshold for *M. bryantii* was 2.4 μM (36). Therefore, the generally higher demand for $H_2$ by *Methanocaldococcus* spp. may be a reflection of higher growth energy requirements for hydrogenotrophic methanogens at hyperthermophilic temperatures, as previously predicted (11). The minimum $H_2$ threshold for methanogenesis at 82 °C in this study was more than 10-fold lower than had been predicted (11), but this reflects the need to refine the parameters used to predict maintenance energies for hyperthermophiles in bioenergetics models through experimentation. For example, increasing the activation energy ($E_a$) in the Hoehler model (11) from 69.4 to 80 kJ mol$^{-1}$ decreases cellular maintenance energies at 82 °C more than 36-fold, which would predict a lower minimum $H_2$ threshold for the organisms. Others have suggested that the $E_a$ is as high as 110 kJ mol$^{-1}$ (37).

**Gas Fluid Chemistry at Axial Volcano and the Endeavour Segment.** The efficacy of our $H_2$-dependent growth kinetic values as an explanation for the general hyperthermophilic methanogen distribution patterns observed in deep-sea hydrothermal vents was tested using high- and low-temperature vent fluids emanating from the seafloor and from hydrothermally active black smoker sulfide chimneys. Using the deep-sea research submarine *Alvin*, the samples were collected in 2008 and 2009 from the caldera of Axial Volcano (depth of 1,520 m) and from the Main, High Rise, and Mothra vent fields along the Endeavour Segment (depth of ~2,200 m). These sites are both on the Juan de Fuca Ridge midocean spreading center in the northeastern Pacific Ocean and are 235 km apart (Fig. S2). Axial Volcano was previously shown to be a site of anomalously high $CH_4$ in low-temperature hydrothermal fluids attributable to subseafloor methanogenesis (38).

Hydrothermal fluids (233 total) ranging in temperature from 2.7 °C (background seawater) to 352 °C were collected with a hydrothermal fluid sampler [HFS (38), 167 samples] and with discrete titanium gas-tight samplers that maintain seafloor hydrostatic pressure (66 samples). The concentrations of $H_2$, $CH_4$, $\Sigma CO_2$, and $Mg^{2+}$ were measured from each gas-tight sample (Table S1). Aqueous dissolved gas concentrations in pure end-member hydrothermal fluids were estimated by extrapolating their measured concentrations in high-temperature gas-tight fluids to a zero $Mg^{2+}$ fluid (Table S1). $H_2$ concentrations in pure hydrothermal fluids were generally higher at Axial Volcano than those from the Endeavour Segment (Fig. 2), except at the ASHES vent field at Axial (Table S1). Estimated $H_2$ concentrations at 82 °C through conserved mixing of end-member hydrothermal fluid with seawater indicate that $H_2$ concentrations would be 82 μmol kg$^{-1}$ ± 43 μmol kg$^{-1}$ (SD) at Axial Volcano and 18 μmol kg$^{-1}$ ± 8 μmol kg$^{-1}$ at the Endeavour Segment. Based on our laboratory studies, $H_2$ concentrations in Axial Volcano hydrothermal fluids are largely above the predicted $K_s$ necessary for hyperthermophilic methanogen growth (except ASHES) but are near or below the minimum $H_2$ threshold in Endeavour Segment fluids. Although $H_2$ drawdown to concentrations below that predicted for the mixing of end-member

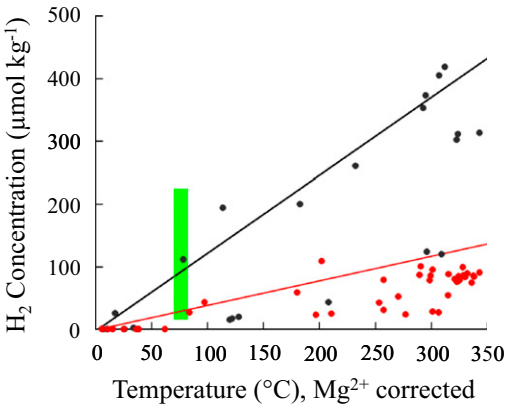


**Fig. 2.** $H_2$ concentrations in hydrothermal fluids collected at various temperatures from Axial Volcano (solid black circle) and the Endeavour Segment (solid red circle). The green box represents the $H_2$ concentrations between 70 °C and 82 °C that support *Methanocaldococcus* spp. growth, as shown in Fig. 1. The black and red lines are for end-member mixing between seawater and the hydrothermal fluid with the highest average gas concentration from Axial Volcano (Caspar vent) and the Endeavour Segment (Hulk vent).

hydrothermal fluid and seawater has been observed previously in diffuse hydrothermal fluids, presumably attributable to microbial consumption (25, 38, 39), this is unlikely to have much effect on the $H_2$ concentration experienced by hyperthermophiles because these organisms are the first to use the $H_2$ derived from the hydrothermal fluid during mixing and cooling.

At Axial Volcano, two vent sites (Virgin Mound and Marker 151) had high-temperature hydrothermal fluids with much higher end-member $CH_4$ and $\Sigma CO_2$ concentrations than all the other vent sites sampled (Table S1). The only other anomalously high $CH_4$ concentrations at Axial Volcano were found in low-temperature (20–34 °C) hydrothermal fluids from the Marker 113 site, which were 17.5 µmol $kg^{-1}$ in a 26 °C gas-tight fluid sample and ranged between 9.0 µM and 66.1 µM in five HFS fluid samples. The end-member $\Sigma CO_2$ concentration (59.6 mmol $kg^{-1}$) for the Marker 113 gas-tight fluid sample was more typical of all other vents at Axial, except Virgin Mound and Marker 151, and its $CH_4/\Sigma CO_2$ ratio was sevenfold higher than the nearest high-temperature fluids in the International District and Coquille vent fields. These findings suggest that the anomalously high methane at Marker 113 had a significant biogenic component. No large $CH_4$ anomalies indicative of extensive methanogenesis were observed in low-temperature hydrothermal fluids from the Endeavour Segment or elsewhere at Axial Volcano.

**Most Probable Number Concentration Estimates, qPCR, and Diversity of Methanogens.** Twenty-eight of the low-temperature (<43 °C) HFS fluid samples and 8 active black smoker chimney samples were used for three-tube most probable number (MPN) estimates of thermophilic and hyperthermophilic methanogens and hyperthermophilic sulfur-reducing heterotrophs. At Axial Volcano, methanogens in our 55 °C and 85 °C MPN estimates were only found in Marker 113 fluids of the five vent sites sampled (Table S2) and from the interior of an active black smoker chimney collected at El Guapo vent (Table S3). At the Endeavour Segment, methanogens were found in only 2 of the 18 low-temperature fluids (S&M and Boardwalk, Table S2) and in 3 of the 6 chimney samples (Table S3). The S&M and Boardwalk vents had estimated $H_2$ concentrations in pure hydrothermal fluids up to 104.1 µmol $kg^{-1}$ and 92.7 µmol $kg^{-1}$, respectively (Table S1), suggesting that they might have $H_2$ concentrations capable of supporting low levels of hyperthermophilic methanogenesis. Hyperthermophilic, anaerobic heterotrophs were found in all but one of the samples at both Axial Volcano and Endeavour, and, on average, they were found at concentrations that were more than 100-fold higher than the hyperthermophilic methanogens (Tables S2 and S3). Because hyperthermophilic heterotrophs and methanogens are both anaerobes and have similar temperature and pH ranges for growth, oxygen, temperature, or pH would not have limited the growth of the methanogens at these sites.

qPCR results showed that low-temperature hydrothermal fluids are dominated by bacteria that comprise 84–98% of the total prokaryotic community (Fig. 3*A*). The methanogen-specific gene *mcrA* (and its paralog *mrtA*) was only found in 3 of 17 low-temperature hydrothermal fluids examined (Table S2). Within these fluids, methanogens comprised only a small fraction of the total archaeal community (0.2–6%) (Fig. 3*A*). No *mcrA* was detected in a background seawater sample (depth of ~1,500 m) from near Axial Volcano. The total gene copies of archaea and bacteria were elevated in all the vents sampled in comparison to this background sample, indicating enrichment of microbes in the vent fluids, as noted from cell count data in low-temperature diffuse fluids (Table S2). *Methanocaldococcus*, *Methanothermococcus*, and *Methanococcus* dominated the *mcrA* sequences found in the three vent fluids from Marker 113 as well as in the 9-m vent at Axial Volcano and in the Easter Island vent at Endeavour (Fig. 3*B*), although relative abundances were nearly 100-fold lower in the Endeavour sample compared with the two Axial samples (Fig. 3*A*). All the *mcrA* sequences from the 9-m vent matched those found at Marker 113, and both vents shared sequences with the Easter

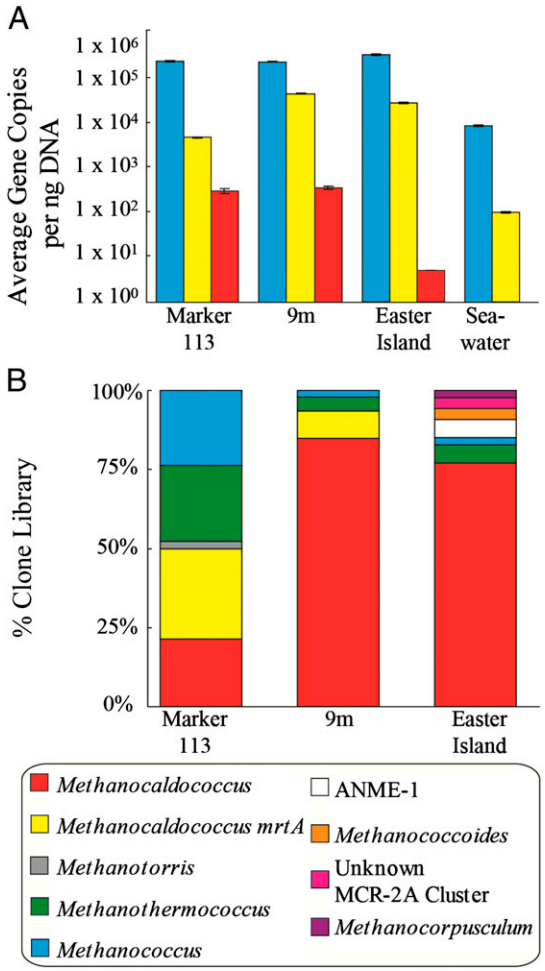


**Fig. 3.** (*A*) Comparison of total gene copy number per nanogram of vent fluid DNA for bacteria 16S rDNA (blue), archaea 16S rDNA (yellow), and *mcrA*/*mrtA* (red). Error bars represent the SEs of average gene copies per nanogram of DNA. (*B*) Comparison of the relative abundance of 6% difference operational taxonomic unit (OTU) groups for all *mcrA*/*mrtA* sequences from all vent fluid samples.

Island vent. A number of uncultivated methanogen groups (ANME-1 and MCR-2A clusters) were found at the Easter Island vent but not at the Marker 113 vent or the 9-m vent. Collectively, our culture-dependent and independent analyses suggest that *Methanocaldococcus* abundances are generally very low at the Endeavour Segment and Axial Volcano, with the exception of the Marker 113 and 9-m sites. This is in agreement with previous culture-dependent and independent surveys at Endeavour (29, 40).

Many low-temperature vent sites (or so-called "diffuse vents") are located just meters away from focused high-temperature fluid flow, possibly confining hyperthermophiles to a thin and shallow subsurface biotic reaction zone, where they would yield little net growth and biogenic fluid chemistry alteration. A vertical temperature profile of the Quest diffuse vent mussel bed near high-temperature venting in the Logatchev Field on the Mid-Atlantic Ridge went from <20 °C to 190 °C within a span of 12 cm (41). The Easter Island and 9-m vents are low-temperature vent sites that are 10–20 m from focused high-temperature venting, whereas S&M and Boardwalk host diffuse venting directly on high-temperature vent structures. In contrast, the Marker 113 vent site at Axial Volcano consists entirely of diffuse venting out of basaltic rock, with the closest known high-temperature venting more than 730 m away (Fig. S2). Marker 113 lies between the Coquille and International District vent fields along the south rift zone, where volcanic eruptions occurred in 1998 (38) and 2011 (42). These fields had high-temperature venting with end-member $H_2$ concentrations up to 384.8 μmol $kg^{-1}$ and 428.1 μmol $kg^{-1}$, respectively, in 2008 and 2009 (Table S1). It is possible that a volumetrically larger subsurface biotic reaction zone heated by a deep magma source and a long residence time of hydrothermal fluids within this zone are important factors leading to anomalously high methane concentrations at the Marker 113 vent.

The minimum $H_2$ concentration for hyperthermophilic methanogen growth determined in this study also appears to hold for other systems (Table S4). Mariner Field at Lau Basin, TOTO Caldera in the Mariana Arc, Brothers Volcano in the Kermadec Arc, and Lucky Strike on the Mid-Atlantic Ridge all had end-member hydrothermal fluid $H_2$ concentrations that were below our growth threshold at 82 °C, and no hyperthermophilic methanogens were found at those sites, although hyperthermophilic, anaerobic heterotrophs were found in significant concentrations (20, 26–28). In contrast, Iheya North Field, Kairei Field, Logatchev Field, and Rainbow Field had end-member $H_2$ concentrations in hydrothermal fluids between 200 μM and 5.9 mM, and hyperthermophilic methanogens were found at these sites in direct proportion to the concentration of $H_2$ present within the system (16, 17, 20). Geochemical evidence for methanogenesis was found in 20.4–24.7 °C diffuse vent fluids from Tubeworm Pillar at 9°N East Pacific Rise, where $H_2$ concentrations had been drawn down to 6–10 μM (25). Genes for Methanococcales uptake hydrogenase were found in <20 °C diffuse fluids from Quest at the Logatchev Field, which had $H_2$ concentrations of 21 μM (41). Therefore, the $H_2$ threshold predicted in this study appears to be broadly applicable as a general explanation of hyperthermophilic methanogen distribution in deep-sea hydrothermal systems.

**$H_2$ Syntrophy Between Methanogens and Heterotrophs.** $H_2$ from high-temperature fluids is unlikely to be the only source of $H_2$ available for methanogenesis in deep-sea hydrothermal vent environments. Some hyperthermophilic, anaerobic heterotrophs produce $H_2$ as an end-product, even when grown with sulfur as a terminal electron acceptor (43). In two of our MPN tubes, methanogens were found growing in coculture with hyperthermophilic heterotrophs where no $H_2$ had been added initially (Tables S2 and S3), suggesting syntrophic (or at least commensal) growth between the two organisms. Hyperthermophilic methanogens have previously been shown to grow solely on the $H_2$ produced by hyperthermophilic heterotrophs, which was proposed to ameliorate growth inhibition by high $H_2$ concentrations in the latter organisms (44, 45). To test for commensalism, *Thermococcus* sp. strain CL1 isolated from the Cleft Segment deep-sea vent site 140 km south of Axial Volcano on the Juan de Fuca Ridge (46) was grown at 82 °C with and without *Methanocaldococcus* sp. strain JH146 from Marker 113 (Fig. 4). The results show initial $H_2$ production, followed by $H_2$ consumption and $CH_4$ production in the mixed culture bottles relative to heterotrophic growth and $H_2$ production alone (Fig. 4*A*). Initial $H_2$ production rates by the heterotroph with and without the methanogen were identical until the onset of methanogenesis. This supports the idea that hyperthermophilic heterotrophs can provide hyperthermophilic methanogens with $H_2$ in situ, especially in otherwise $H_2$-limited hydrothermal vent systems.

FISH staining and microscopy for *Thermococcus* and *Methanocaldococcus* species in our cocultures suggest that these organisms grow in aggregates, where the heterotrophs significantly outnumber the methanogens (Fig. 4*B*). Previous estimates of $H_2$ production rates by a hyperthermophilic heterotroph (43) and $H_2$ consumption by *Methanocaldococcus* strain JH146, based on a 4:1 $H_2$ consumption-to-$CH_4$ production ratio, suggest that 27–47 hyperthermophilic heterotrophs could produce enough $H_2$ to sustain a single *Methanocaldococcus* cell (47). This would be possible at Axial Volcano and the Endeavour Segment, given the relative and colocalized abundances of hyperthermophilic heterotrophs and methanogens in our MPN results (Tables S2 and S3). $H_2$ syntrophy would be constrained by the availability of organic material, which may flow in from mesophilic bacteria and macrofauna that colonize the cooler outer surfaces of active hydrothermal sulfide chimneys (often only a few centimeters away from the hyperthermophiles in our samples) and the basalt seafloor in regions of diffuse venting. The exterior surfaces of active sulfide chimneys on the Juan de Fuca Ridge are often

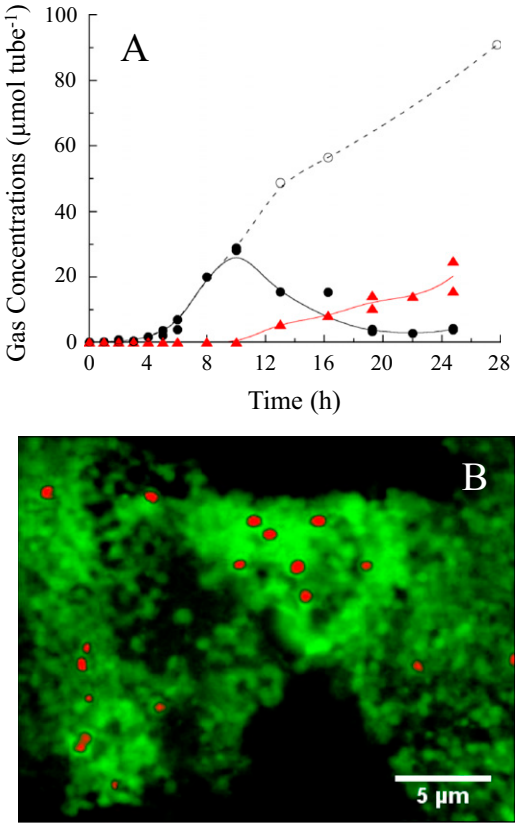


**Fig. 4.** (*A*) $H_2$ production by *Thermococcus* strain CL1 when grown at 82 °C with (solid black circle) and without (open black circle) *Methanocaldococcus* strain JH146 and $CH_4$ production by strain JH146 solid red triangle) when grown in coculture with strain CL1. Concentrations of $H_2$ and $CH_4$ are in micromoles per Balch tube. (*B*) FISH staining of strains CL1 (green) and JH146 (red) grown in coculture.

heavily colonized by *Paralvinella* spp. polychaete worms that form tubes below the surface, and hyperthermophilic heterotrophs were found on the worms and in their tubes and associated substratum (46, 48). Hyperthermophilic methanogens may serve as primary producers in deep-sea vents only when abiotically derived $H_2$ concentrations are sufficiently high, such as after a volcanic eruption or in ultramafic rock-hosted vent sites.

**Conclusion.** Although there are several factors that can limit the growth of hyperthermophiles in deep-sea hydrothermal vents (e.g., temperature, pH, redox potential), the results of this study demonstrate that $H_2$ availability at concentrations of at least 17–23 μM at hyperthermophile growth temperatures is one of the key determinants for the presence of *Methanocaldococcus* species. This predicted value is a minimum threshold, given the otherwise optimal growth conditions in our bioreactor study, and might increase with differences in growth energy costs under less optimal environmental conditions. Our results also point to the importance of commensalism or syntrophy between hyperthermophile species in a system that is energy-limited. Ultimately, our ability to model the growth and metabolite production rates of methanogens and other microbes at various temperatures will enable us to make better predictions regarding the habitability and bioenergetics of various regions of the subseafloor. Biogeochemical models of the microbial impact on carbon flux and chemical cycling within the deep sea and the ocean crust will then require the development of reactive transport models for the subseafloor that further integrate additional physical, chemical, and biological parameters.

## Materials and Methods

**Growth Media and Organisms Used.** The growth media for the hyperthermophilic methanogens, the heterotrophic sulfur reducers, and the coculture of methanogens and heterotrophs are based on those described previously and are defined in *SI Materials and Methods*. *M. jannaschii* DSM 2661 was purchased from Deutsche Sammlung von Mikroorganismen und Zellkulturen (DSM). *Methanocaldococcus* strains JH146 and JH123 and *Thermococcus* strain CL1 are from the culture collection in the laboratory of one of the authors (J.F.H.).

For the $H_2$ limitation experiments, a 2-L bioreactor with gas flow control, incubation temperatures of 82 °C and 70 °C (±0.1 °C), and a pH of 6.0 (±0.1 pH unit) was prepared with 1.7 L of "282mod" medium. The reactor was degassed through a submerged fritted bubbler with a mixture of $CO_2$ (7.5 mL of gas $min^{-1}$), $H_2$, and argon. The $H_2$ gas flow rate and $H_2$ concentration varied for different growth kinetics experiments: 2.3 mL $min^{-1}$ (16.5 μM $H_2$), 3 mL $min^{-1}$ (22 μM $H_2$), 6 mL $min^{-1}$ (45 μM $H_2$), 12 mL $min^{-1}$ (90 μM $H_2$), 24 mL $min^{-1}$ (180 μM $H_2$), and 30 mL $min^{-1}$ (225 μM $H_2$). For 10 μM $H_2$, 2.2 mL $min^{-1}$ of $H_2$/argon (5:95 ratio) was used. Argon was added to balance the total gas flow at 37.5 mL of gas $min^{-1}$. The aqueous $H_2$ concentration in the reactor at all $H_2$ flow rate settings and both incubation temperatures was measured by drawing ~25 mL of fluid from the bottom of the reactor directly into anoxic 60-mL serum bottles and measuring the head-space gas with a gas chromatograph. DTT (4.8 mM) was added to reduce the bioreactor fully. The reactor was inoculated with 25 mL of a logarithmic growth-phase culture of *M. jannaschii*, strain JH146, or strain JH123. During growth, samples were drawn from the reactor and cell concentrations were determined using phase-contrast light microscopy and a Petroff–Hausser counting chamber. Each growth kinetic experiment for each organism was run in duplicate or triplicate.

**Field Sampling.** Samples were collected in August–September 2008 and in June 2009 from the Main, High Rise, and Mothra vent fields along the Endeavour Segment and from the caldera of Axial Volcano, both on the Juan de Fuca Ridge in the northeastern Pacific Ocean (Fig. S2), using the deep-sea research submarine *Alvin*. For each vent fluid sampled, the maximum temperature of the fluid was measured using a temperature probe attached to the *Alvin*. The HFS pumped vent fluid through a titanium nozzle and measured the temperature of the fluid at 1 Hz just inside the nozzle. Fluid sample containers were either collapsible Tedlar plastic bags with valves within rigid housings, PVC piston samplers, or titanium piston samplers. All samplers have check valves to prevent the samples from leaking out or being drawn out of the containers. Sample valves were closed on arrival on deck, and samples were stored under refrigeration until processed. For DNA analysis, the HFS pulled 1–4 L of low-temperature fluid through a Sterivex-GP (0.22-μm pore size, Millipore) filter in situ at a flow rate of ~150 mL $min^{-1}$. These filters were frozen immediately at −80 °C on vehicle recovery.

**Fluid Chemistry Analyses.** Concentrations of $H_2$, $CH_4$, $\Sigma CO_2$, and $Mg^{2+}$ in each of the gas-tight fluid samples were determined as previously described (24, 38). $Mg^{2+}$-corrected sampling temperatures for the gas-tight fluid samples were based on the proportion of seawater $Mg^{2+}$ measured in the sample relative to the maximum fluid temperature measured for that fluid immediately before sampling. Subsamples of HFS fluids were taken directly from the collapsible bags and piston samples into syringes without exposure to air for shipboard analysis of $H_2$ and $CH_4$ using gas chromatography. If a gas headspace was present, the gas-phase and liquid-phase volumes were measured and both phases were sampled and analyzed by gas chromatography.

**MPN Estimates.** Once on deck, 50 mL of 28 different HFS fluid samples were transferred by syringe into sealed anoxic serum bottles, which were then flushed with argon and reduced with 0.25% each of cysteine·HCl and $Na_2S{\cdot}9H_2O$. Five black smoker chimney samples were also collected. A total of 12–14 g of the soft porous wurtzite-sphalerite–rich material from the interior of the chimney and, when possible, 5–8 g of the scraped hard-silicate–enriched exterior of the chimney were added to separate degassed serum bottles containing 50 mL of sterile artificial seawater composed of the salts in DSM medium 141. These were then flushed with argon and reduced with 0.25% each of cysteine·HCl and $Na_2S{\cdot}9H_2O$. A detailed description of the MPN estimates is provided in the supplemental material.

**Sequencing of *mcrA*.** DNA was extracted as previously described (49), and details of the sequencing are described further in *SI Materials and Methods*. Amplification of *mcrA* and its paralog *mrtA* was performed using both the ME primer set (50) and the MCR primer set (51). Following PCR, the three reactions for each sample were combined, purified, and ligated into pCR4-TOPO vectors. For each library, 48–96 clones were randomly selected, grown overnight at 37 °C, and collected by centrifugation. Plasmid DNA was isolated and sequenced bidirectionally with primers T3 and T7 using AB BigDye3.1 (Applied Biosystems) chemistry and analyzed with an AB 3730xl Genetic Analyzer (Applied Biosystems). The GenBank nucleotide sequence accession numbers for the sequences in this study are HQ635140 through HQ635763.

**qPCR of *mcrA*.** qPCR TaqMan assays (52, 53) were used to determine the abundance of bacterial and archaeal 16S rRNA genes in environmental vent fluids as previously described (54). *mcrA*/*mrtA* gene copies were determined by qPCR SYBR assays run simultaneously with TaqMan assays. Multiple alignments of *mcrA*/*mrtA* sequences obtained from this study were used to design a previously undescribed forward primer designated qmcrA-F-ALT (5′-GAR GAC CAC TTY GGH GGT TC-3′). Used in combination with the reverse primer ML-R (50), the resulting amplicon was 265 bp. Primer specificity was confirmed by amplifying, cloning, and sequencing environmental sample A4-Sx12 from Axial Volcano. Plasmid DNA standards were extracted from the Endeavour Segment Easter Island vent fluid sample, purified, and linearized using the WizardPlus SV Minipreps DNA Purification System (Promega). A 1:10 dilution series of the plasmid beginning with an initial concentration of ~0.037 ng $\mu L^{-1}$ was used to produce standard curves with $R^2$ values greater than 0.999 and efficiencies ranging from 91–96%. Each 20-μL reaction contained Power SYBR Green PCR Master Mix (Applied Biosystems), 1 unit of AmpErase Uracil *N*-glycosylase (Applied Biosystems), forward and reverse primers at optimized concentrations of 6 μM, diethylpyrocarbonate-treated water, and 2 μL of DNA template. Reaction conditions were identical to those for TaqMan assays except for the addition of a melting curve analysis to determine amplicon specificity with temperature increases from 60 °C to 95 °C in increments of 0.3 °C every 15 s.

**Coculture of Methanogen and Heterotroph.** To test for $H_2$ commensalism, *Thermococcus* sp. strain CL1 (46) and *Methanocaldococcus* sp. strain JH146 were grown in modified DSM 399–141 medium (*SI Materials and Methods*) at 82 °C. A coculture was established and maintained through several transfers. Growth kinetics experiments were conducted with concomitant $H_2$ and $CH_4$ measurements for each strain grown individually and in coculture. For cocultures, Balch tubes containing 10 mL of media were inoculated with 0.1 mL of logarithmically growing coculture and 0.05 mL of logarithmically growing methanogen pure culture. During growth, duplicate tubes were permanently removed from incubation at various time points. Once cooled to room temperature, the volume of gas within each tube was measured with a pressure-lock syringe. $H_2$ and $CH_4$ were measured using gas chromatography. For visualization of cellular interactions, subsamples of coculture

experiments were analyzed with FISH using the probes Tcoc164 (5′-CAV RCC TAT GGG GGA TTA GC-3′) and MC504 (5′-GGC TGC TGG CAC CGG ACT TGC CCA-3′) for Thermococcales and Methanocaldococcaceae, respectively, as described previously (55, 56) and in *SI Materials and Methods*.

**ACKNOWLEDGMENTS.** We thank Dmitry Tokar, Sabrina Parise, Samantha Zelin, and the personnel onboard the R/V *Atlantis* and DSV *Alvin* for technical assistance. This study was supported by the National Science Foundation Division of Ocean Sciences Grant OCE-0732611 (to J.F.H.); National Science Foundation Grant OCE-0731947 (to D.A.B. and M.D.L.); and National Science Foundation Grant OCE-0929167, National Aeronautics and Space Administration Astrobiology Institute Cooperative Agreement NNA04CC04A Director's Discretionary Fund, and a L'Oreal USA Fellowship (to J.A.H.). A.Y.M. was partially supported by the National Aeronautics and Space Administration Planetary Biology Internship Program. This publication is partially funded by the Joint Institute for the Study of the Atmosphere and Ocean under National Oceanic and Atmospheric Administration Cooperative Agreement NA17RJ1232, Contribution 1897. This is National Oceanic and Atmospheric Administration Pacific Marine Environmental Laboratory Contribution 3797.

1. Parkes RJ, et al. (1994) Deep bacterial biosphere in Pacific Ocean sediments. *Nature* 271:410–413.
2. Lipp JS, Morono Y, Inagaki F, Hinrichs K-U (2008) Significant contribution of Archaea to extant biomass in marine subsurface sediments. *Nature* 454:991–994.
3. Whitman WB, Coleman DC, Wiebe WJ (1998) Prokaryotes: The unseen majority. *Proc Natl Acad Sci USA* 95:6578–6583.
4. Heberling C, Lowell RP, Liu L, Fisk MR (2010) Extent of the microbial biosphere in the oceanic crust. *Geochem Geophys Geosyst* 11:Q08003.
5. D'Hondt S, Rutherford S, Spivack AJ (2002) Metabolic activity of subsurface life in deep-sea sediments. *Science* 295:2067–2070.
6. D'Hondt S, et al. (2004) Distributions of microbial activities in deep subseafloor sediments. *Science* 306:2216–2221.
7. Chapelle FH, et al. (2002) A hydrogen-based subsurface microbial community dominated by methanogens. *Nature* 415:312–315.
8. Moser DP, et al. (2005) *Desulfotomaculum* and *Methanobacterium* spp. dominate a 4- to 5-kilometer-deep fault. *Appl Environ Microbiol* 71:8773–8783.
9. Lin L-H, et al. (2006) Long-term sustainability of a high-energy, low-diversity crustal biome. *Science* 314:479–482.
10. McCollom TM, Shock EL (1997) Geochemical constraints on chemolithoautotrophic metabolism by microorganisms in seafloor hydrothermal systems. *Geochim Cosmochim Acta* 61:4375–4391.
11. Hoehler TM (2004) Biological energy requirements as quantitative boundary conditions for life in the subsurface. *Geobiology* 2:205–215.
12. Shock EL, Holland ME (2007) Quantitative habitability. *Astrobiology* 7:839–851.
13. Amend JP, McCollom TM, Hentscher M, Bach W (2011) Catabolic and anabolic energy for chemolithoautotrophs in deep-sea hydrothermal systems hosted in different rock types. *Geochim Cosmochim Acta* 75:5736–5748.
14. Huber JA, Butterfield DA, Baross JA (2002) Temporal changes in archaeal diversity and chemistry in a mid-ocean ridge subseafloor habitat. *Appl Environ Microbiol* 68:1585–1594.
15. Higashi Y, et al. (2004) Microbial diversity in hydrothermal surface to subsurface environments of Suiyo Seamount, Izu-Bonin Arc, using a catheter-type in situ growth chamber. *FEMS Microbiol Ecol* 47:327–336.
16. Takai K, et al. (2004) Geochemical and microbiological evidence for a hydrogen-based, hyperthermophilic subsurface lithoautotrophic microbial ecosystem (HyperSLiME) beneath an active deep-sea hydrothermal field. *Extremophiles* 8:269–282.
17. Nakagawa S, et al. (2005) Variability in microbial community and venting chemistry in a sediment-hosted backarc hydrothermal system: Impacts of subseafloor phase-separation. *FEMS Microbiol Ecol* 54:141–155.
18. Nercessian O, Bienvenu N, Moreira D, Prieur D, Jeanthon C (2005) Diversity of functional genes of methanogens, methanotrophs and sulfate reducers in deep-sea hydrothermal environments. *Environ Microbiol* 7:118–132.
19. Perner M, et al. (2007) The influence of ultramafic rocks on microbial communities at the Logatchev hydrothermal field, located 15 degrees N on the Mid-Atlantic Ridge. *FEMS Microbiol Ecol* 61:97–109.
20. Flores GE, et al. (2011) Microbial community structure of hydrothermal deposits from geochemically different vent fields along the Mid-Atlantic Ridge. *Environ Microbiol* 13:2158–2171.
21. Roussel EG, et al. (2011) Comparison of microbial communities associated with three Atlantic ultramafic hydrothermal systems. *FEMS Microbiol Ecol* 77:647–665.
22. Holden JF, Summit M, Baross JA (1998) Thermophilic and hyperthermophilic microorganisms in 3-30 °C hydrothermal fluids following a deep-sea volcanic eruption. *FEMS Microbiol Ecol* 25:33–41.
23. Von Damm KL, Lilley MD (2004) *The Subseafloor Biosphere at Mid-Ocean Ridges*, eds Wilcock WSD, DeLong EF, Kelley DS, Baross JA, Cary SC (American Geophysical Union, Washington, DC), pp 245–268.
24. Proskurowski G, Lilley MD, Olson EJ (2008) Stable isotopic evidence in support of active microbial methane cycling in low-temperature diffuse flow vents at 9°50°N East Pacific Rise. *Geochim Cosmochim Acta* 72:2005–2023.
25. Hentscher M, Bach W (2012) Geochemically induced shifts in catabolic energy yields explain past ecological changes of diffuse vents in the East Pacific Rise 9°50′N area. *Geochem Trans* 13:2.
26. Nakagawa T, et al. (2006) Geomicrobiological exploration and characterization of a novel deep-sea hydrothermal system at the TOTO caldera in the Mariana Volcanic Arc. *Environ Microbiol* 8:37–49.
27. Takai K, et al. (2008) Variability in the microbial communities and hydrothermal fluid chemistry at the newly discovered Mariner hydrothermal field, southern Lau Basin. *J Geophys Res* 113:G02031.
28. Takai K, et al. (2009) Variability in microbial communities in black smoker chimneys at the NW Caldera vent field, Brothers Volcano, Kermadec Arc. *Geomicrobiol J* 26:552–569.
29. Ver Eecke HC, Kelley DS, Holden JF (2009) Abundances of hyperthermophilic autotrophic Fe(III) oxide reducers and heterotrophs in hydrothermal sulfide chimneys of the northeastern Pacific Ocean. *Appl Environ Microbiol* 75:242–245.
30. Tijhuis L, Van Loosdrecht MCM, Heijnen JJ (1993) A thermodynamically based correlation for maintenance gibbs energy requirements in aerobic and anaerobic chemotrophic growth. *Biotechnol Bioeng* 42:509–519.
31. Amend JP, Shock EL (2001) Energetics of overall metabolic reactions of thermophilic and hyperthermophilic Archaea and bacteria. *FEMS Microbiol Rev* 25:175–243.
32. Miller JF, Shah NN, Nelson CM, Ludlow JM, Clark DS (1988) Pressure and temperature effects on growth and methane production of the extreme thermophile *Methanococcus jannaschii*. *Appl Environ Microbiol* 54:3039–3042.
33. Miller JF, Nelson CM, Ludlow JM, Shah NN, Clark DS (1989) High pressure-temperature bioreactor: Assays of thermostable hydrogenase with fiber optics. *Biotechnol Bioeng* 34:1015–1021.
34. Boonyaratanakornkit BB, Miao LY, Clark DS (2007) Transcriptional responses of the deep-sea hyperthermophile *Methanocaldococcus jannaschii* under shifting extremes of temperature and pressure. *Extremophiles* 11:495–503.
35. Robinson JA, Tiedje JM (1984) Competition between sulfate-reducing and methanogenic bacteria for $H_2$ under resting and growing conditions. *Arch Microbiol* 137: 26–32.
36. Karadagli F, Rittmann BE (2005) Kinetic characterization of *Methanobacterium bryantii* M.o.H. *Environ Sci Technol* 39:4900–4905.
37. Price PB, Sowers T (2004) Temperature dependence of metabolic rates for microbial growth, maintenance, and survival. *Proc Natl Acad Sci USA* 101:4631–4636.
38. Butterfield DA, et al. (2004) *The Subseafloor Biosphere at Mid-Ocean Ridges*, eds Wilcock WSD, DeLong EF, Kelley DS, Baross JA, Cary SC (American Geophysical Union, Washington, DC), pp 269–289.
39. Wankel SD, et al. (2011) Influence of subsurface biosphere on geochemical fluxes from diffuse hydrothermal fluids. *Nat Geosci* 4:461–468.
40. Zhou H, et al. (2009) Microbial diversity of a sulfide black smoker in main endeavour hydrothermal vent field, Juan de Fuca Ridge. *J Microbiol* 47:235–247.
41. Perner M, Petersen JM, Zielinski F, Gennerich HH, Seifert R (2010) Geochemical constraints on the diversity and activity of $H_2$-oxidizing microorganisms in diffuse hydrothermal fluids from a basalt- and an ultramafic-hosted vent. *FEMS Microbiol Ecol* 74:55–71.
42. Chadwick WW, Jr., Nooner SL, Butterfield DA, Lilley MD (2012) Seafloor deformation and forecasts of the April 2011 eruption at Axial Seamount. *Nat Geosci* 5:474–477.
43. Oslowski DM, Jung JH, Seo DH, Park CS, Holden JF (2011) Production of hydrogen from α-1,4- and β-1,4-linked saccharides by marine hyperthermophilic Archaea. *Appl Environ Microbiol* 77:3169–3173.
44. Bonch-Osmolovskaya EA, Stetter KO (1991) Interspecies hydrogen transfer in cocultures of thermophilic *Archaea*. *Syst Appl Microbiol* 14:205–208.
45. Johnson MR, et al. (2006) The *Thermotoga maritima* phenotype is impacted by syntrophic interaction with *Methanococcus jannaschii* in hyperthermophilic coculture. *Appl Environ Microbiol* 72:811–818.
46. Holden JF, et al. (2001) Diversity among three novel groups of hyperthermophilic deep-sea *Thermococcus* species from three sites in the northeastern Pacific Ocean. *FEMS Microbiol Ecol* 36:51–60.
47. Ver Eecke HC (2011) Growth kinetics and constraints related to metabolic diversity and abundances of hyperthermophiles in deep-sea hydrothermal vents. PhD dissertation (Univ of Massachusetts, Amherst, MA).
48. Pagé A, et al. (2004) Microbial diversity associated with a *Paralvinella sulfincola* tube and the adjacent substratum on an active deep-sea vent chimney. *Geobiology* 2: 225–238.
49. Huber JA, et al. (2007) Microbial population structures in the deep marine biosphere. *Science* 318:97–100.
50. Hales BA, et al. (1996) Isolation and identification of methanogen-specific DNA from blanket bog peat by PCR amplification and sequence analysis. *Appl Environ Microbiol* 62:668–675.
51. Luton PE, Wayne JM, Sharp RJ, Riley PW (2002) The *mcrA* gene as an alternative to 16S rRNA in the phylogenetic analysis of methanogen populations in landfill. *Microbiology* 148:3521–3530.
52. Nadkarni MA, Martin FE, Jacques NA, Hunter N (2002) Determination of bacterial load by real-time PCR using a broad-range (universal) probe and primers set. *Microbiology* 148:257–266.
53. Takai K, Horikoshi K (2000) Rapid detection and quantification of members of the archaeal community by quantitative PCR using fluorogenic probes. *Appl Environ Microbiol* 66:5066–5072.
54. Huber JA, et al. (2010) Isolated communities of Epsilonproteobacteria in hydrothermal vent fluids of the Mariana Arc seamounts. *FEMS Microbiol Ecol* 73:538–549.
55. Crocetti G, Murto M, Björnsson L (2006) An update and optimisation of oligonucleotide probes targeting methanogenic Archaea for use in fluorescence in situ hybridisation (FISH). *J Microbiol Methods* 65:194–201.
56. Rusch A, Amend JP (2004) Order-specific 16S rRNA-targeted oligonucleotide probes for (hyper)thermophilic archaea and bacteria. *Extremophiles* 8:357–366.